Published in final edited form as:
Neuroscience. 2012 November 8; 224C: 145–159. doi:10.1016/j.neuroscience.2012.08.021.

ULTRASTRUCTURAL ANALYSIS OF RAT VENTROLATERAL PERIAQUEDUCTAL GRAY PROJECTIONS TO THE A5 CELL GROUP

Dusica Bajic[a,1], **Elisabeth J. Van Bockstaele**[b], and **Herbert K. Proudfit**[a]

[a]Department of Pharmacology, University of Illinois at Chicago, 835 S. Wolcott Avenue, Chicago, IL 60612, USA

[b]Department of Pathology, Anatomy and Cell Biology, Thomas Jefferson University, 1020 Locust Street, Philadelphia, Pennsylvania 19107, USA

Abstract

Stimulation of neurons in the ventrolateral periaqueductal gray (PAG) produces antinociception as well as cardiovascular depressor responses that are mediated in part by pontine noradrenergic neurons. A previous report using light microscopy has described a pathway from neurons in the ventrolateral PAG to noradrenergic neurons in the A5 cell group that may mediate these effects. The present study used anterograde tracing and electron microscopic analysis to provide more definitive evidence that neurons in the ventrolateral PAG form synapses with noradrenergic and non-catecholaminergic A5 neurons in Sasco Sprague-Dawley rats. Deposits of anterograde tracer, biotinylated dextran amine, into the rat ventrolateral PAG labeled a significant number of axons in the region of the rostral subdivision of the A5 cell group, and a relatively lower number in the caudal A5 cell group. Electron microscopic analysis of anterogradely-labeled terminals in both rostral (n=127) and caudal (n=70) regions of the A5 cell group indicated that approximately 10% of these form synapses with noradrenergic dendrites. In rostral sections, about 31% of these were symmetric synapses, 19% were asymmetric synapses, and 50% were membrane appositions without clear synaptic specializations. In caudal sections, about 22% were symmetric synapses, and the remaining 78% were appositions. In both rostral and caudal subdivisions of the A5, nearly 40% of the anterogradely-labeled terminals formed synapses with non-catecholaminergic dendrites, and about 45% formed axoaxonic synapses. These results provide direct evidence for a monosynaptic pathway from neurons in the ventrolateral PAG to noradrenergic and non-catecholaminergic neurons in the A5 cell group. Further studies should evaluate if this established monosynaptic pathway may contribute to the cardiovascular depressor effects or the analgesia produced by activation of neurons in the ventrolateral PAG.

Keywords

Anterograde tracer; Biotinylated dextran amine; Electron microscopy; Synapse; Tyrosine hydroxylase; Ultrastructure

[1]**Corresponding Author**: Department of Anesthesiology, Perioperative and Pain Medicine Boston Children's Hospital, Bader 3 300 Longwood Avenue Boston, MA 02115 Tel: 617-355-7737 Fax: 617-730-0894 dusica.bajic@childrens.harvard.edu.

CONFLICT OF INTEREST STATEMENT There are no conflicts of interest.

1. INTRODUCTION

The periaqueductal gray region (PAG), which extends throughout the midbrain surrounding the cerebral aqueduct (Paxinos and Watson, 1997), has been divided into several longitudinal zones or columns on the basis of cytoarchitecture, chemoarchitecture, and connections (Bandler et al., 1991, Bandler and Depaulis, 1991, Bandler and Shipley, 1994). The major autonomic connections of the PAG are within the ventrolateral zone that integrates a behavioral response characterized by quiescence, hyporeactivity, hypotension and bradycardia (Bandler and Depaulis, 1991). Excitation of neurons within this discrete ventrolateral region evokes a behavioral reaction that is seemingly identical to that evoked by pain arising from deep structures (Keay et al., 1994). Also, several studies have demonstrated that the ventrolateral PAG is selectively activated by deep pain (Keay et al., 1994, Clement et al., 1996, Clement et al., 2000) and hypotension (Murphy et al., 1995). Furthermore, the ventrolateral PAG is a major brainstem site involved in mediating antinociceptive effects (Fardin et al., 1984a, b), as well as a major site at which opioids act to produce analgesia (Yaksh and Rudy, 1978, Jones, 1992).

The sympathetic inhibition and antinociception produced by stimulation of the ventrolateral PAG are mediated in part by activation of spinally-projecting neurons in the ventromedial medulla (Gebhart and Randich, 1990, Jones, 1992, Lovick, 1993). However, several anatomical and pharmacological studies suggest that projections from the ventrolateral PAG to the noradrenergic neurons in the A5 cell group may contribute to behavioral responses and antinociception produced by activating neurons in the ventrolateral PAG. Our previous anterograde tracing studies (Bajic and Proudfit, 1999) have demonstrated that neurons in the ventrolateral PAG provide a moderately dense innervation of noradrenergic neurons in the A5 cell group. Furthermore, noradrenergic neurons in the A5 cell group have been shown to innervate the intermediolateral cell column in thoracic spinal cord segments (Loewy et al., 1979, Byrum and Guyenet, 1987, Romagnano et al., 1991, Clark and Proudfit, 1993, Bruinstroop et al., 2012), as well as spinal cord dorsal horn (Clark and Proudfit, 1993, Bruinstroop et al., 2012), where numerous nociceptive neurons are located (Light, 1992). In addition, stimulation of A5 neurons with microinjection of glutamate produces a depressor effect (Stanek et al., 1984, Burnett and Gebhart, 1991). Furthermore, microelectrophoretically applied norepinephrine inhibits single sympathetic preganglionic neurons in the thoracic segment of the spinal cord activated by electrical stimulation of a brainstem excitatory region (Coote et al., 1981), implicating descending noradrenergic projection from the A5 cell group in the regulation of cardiovascular reflexes. Similarly, both electrical (Miller and Proudfit, 1990) and chemical (Burnett and Gebhart, 1991) stimulation of sites near the A5 cell group can produce antinociception that is reduced by intrathecal injection of alpha2-adrenoceptor antagonists. Finally, norepinephrine appears to directly modulate the activity of spinothalamic tract neurons, because noradrenergic axon terminals form synapses with identified spinothalamic tract neurons (Westlund et al., 1990) and unidentified dorsal horn neurons (Hagihira et al., 1990, Doyle and Maxwell, 1991a, b), suggesting a role of A5 cell group in modulating nociception. Although previous anterograde tracing studies (Bajic and Proudfit, 1999) provided anatomical evidence that neurons in the ventrolateral PAG project to the region containing noradrenergic neurons of the A5 cell group, these studies did not demonstrate synapses formed by ventrolateral PAG neurons with noradrenergic and non-catecholaminergic A5 neurons. In this study, we used the anterograde tracing technique combined with tyrosine hydroxylase (TH)-immunoreactivity, to evaluate the existence and extent of ventrolateral PAG projections to the A5 cell group. Therefore, the major goal of the present study was to provide ultrastructural evidence that neurons in the ventrolateral PAG form direct synaptic contacts with noradrenergic neurons of the A5 cell group. Also, the catecholamine neurons that comprise the A5 cell group are divided into two distinctive clusters (Dahlstroem and Fuxe,

1964, Lyons and Grzanna, 1988, Clark and Proudfit, 1993). A rostral subdivision is located caudal to the ventral nucleus of the lateral lemniscus at the level of the trigeminal motor nucleus, whereas a caudal subdivision is located lateral and dorsal to the superior olivary complex. Therefore, to evaluate the existence and extent of projections of neurons in the ventrolateral PAG to the A5 cell group, both rostral and caudal subdivisions of the A5 cell group were analyzed separately. The anterograde tracer biotinylated dextran amine (BDA) was iontophoretically deposited into sites in the ventrolateral PAG and electron microscopic analysis was used to visualize synapses formed by anterogradely-labeled terminals and profiles that exhibited immunoreactivity for the catecholamine synthesizing enzyme, TH. The results of this study provide direct ultrastructural evidence for a monosynaptic pathway from neurons in the ventrolateral PAG to noradrenergic as well as non-catecholaminergic dendrites in the A5 cell group.

2. EXPERIMENTAL PROCEDURES

2.1. Animal Care and Use

The Animal Care and Use Committees of the University of Illinois and Thomas Jefferson University where the studies were performed approved the experimental protocols for the use of vertebrate animals in this study. The experiments were conducted according to the National Institutes of Health Guide for the Care and Use of Laboratory Animals (NIH Publications No. 80-23, revised 1996). All efforts were made to minimize the number of animals used and their suffering.

2.2. Anterograde Tracer Iontophoresis and Tissue Fixation

Ten female and six male Sprague-Dawley rats (250-300 g; Sasco, Madison, WI) were injected with anterograde tracer BDA, and two female animals were selected for ultrastructural analysis. Animals were deeply anesthetized with pentobarbital (50 mg/kg) and surgically prepared using aseptic techniques. A glass micropipette (1.2 mm outer diameter, with filament; World Precision Instruments, Inc., Sarasota, FL) with a tip diameter of 15-20 μm was filled with a 10% solution of the anterograde tracer BDA (10,000 MW; D-1956, Molecular Probes, Eugene, OR) in saline and lowered to the appropriate target site in the ventrolateral PAG using the following stereotaxic coordinates relative to lambda: anterior, 0.0 mm; lateral, 0.5 mm; and ventral, 5.7 mm to the surface of the brain. The incisor bar was set at −2.5 mm. BDA was iontophoretically deposited using 5 μA positive current pulses of 500 msec duration at a rate of 0.5 Hz for 30 minutes. The pipette remained in place for 60 seconds after the injection to minimize diffusion of the tracer along the electrode track. A period of 12-18 days was allowed to tracer transport. Animals were then deeply anesthetized with pentobarbital (70 mg/kg, intraperitoneally) and transcardially perfused with: (1) 10 ml of heparinized saline (1000 units/ml; Elkins-Sinn, Inc., Cherry Hill, NH) at a speed of 100 ml/min, followed by (2) 100 ml of 3.75% acrolein (Electron Microscopy Sciences, Fort Washington, PA) and 2% paraformaldehyde in 0.1M phosphate buffer (PB) adjusted to pH 7.4 and perfused at the same speed, and (3) 100 ml of 2% paraformaldehyde in 0.1M PB adjusted to pH 7.4 and perfused at a speed of 100 ml/min; an additional 100 ml of a latter solution was perfused at a speed of 60 ml/min. Following perfusion, fixed brains were removed, cut into blocks and post-fixed in 2% paraformaldehyde overnight. Finally, brain blocks were immersed in cold 0.1M PB and 40 μm transverse sections were cut on a Vibratome. Freely floating sections were then processed for immunocytochemistry.

2.3. Immunocytochemical Tissue Processing

Tissue sections were processed for visualization of BDA using methods described in previous reports (Bajic et al., 2000, Bajic et al., 2001). Tissue sections were rinsed for 5

minutes in 0.1 M PB (pH 7.4), 30 minutes in 1.5% sodium-borohydride in 0.1M PB solution, and 10 minutes in 0.1 M Tris-buffered saline (TBS, pH 7.6). Sections were then incubated for 1.5-2 hours in a solution containing avidin-biotin complex (Elite Standard Vectastain ABC Kit, PK-6100, Vector Laboratories, Inc.) at room temperature, followed by two 10 minutes rinses in 0.1M TBS (pH 7.6). Brown peroxidase reaction product was produced by incubation of sections for 4-5 minutes in a solution containing 22 mg of 3,3′-diaminobenzidine (Aldrich, Milwaukee, WI) and 20 ml of 30% hydrogen peroxide in 100 ml of 0.1 M TBS (pH 7.6).

Following the processing for visualization of BDA, sections were incubated overnight in a solution containing mouse antisera directed against TH (Incstar Corp., Stillwater, MN) that was diluted 1:5,000 with 0.1 M TBS and contained 0.1% bovine serum albumin (BSA). After several rinses in 0.1 M TBS and 0.01 M phosphate buffer saline (PBS, pH 7.4), sections were placed in a blocking solution containing 0.01 M PBS with 0.2% gelatin (Gelatin, IGSS quality, Amersham Life Sciences, Piscataway, NJ) and 0.8% BSA for 10 minutes. Sections were then incubated for 2 hours in a solution containing goat anti-mouse secondary antibody conjugated to 1 nm gold particles (Auro Probe One GAM, RPH 471, Amersham Corp., Arlington Heights, IL) diluted 1:50 with the blocking solution described above. Sections were rinsed again for 10 minutes in the blocking solution, three times for 10 minutes in 0.01 M PBS, and for 10 minutes in 2% glutaraldehyde. After a 10 minute rinse in 0.01 M PBS, sections were washed in 0.2 M sodium citrate buffer (pH 7.4) to remove phosphate ions that could contribute to the nonspecific precipitation of silver. The optimal time for silver enhancement (Intense M Silver Enhancement kit, RPN 491, Amersham Corp.) was determined to be 15-20 minutes and transferring the sections to 0.2 M sodium citrate buffer stopped the reaction. This processing produced black staining of TH-immunoreactive (TH-ir) neurons in the A5 cell group. All incubations and washes were carried out at room temperature with gentle agitation. Following the silver intensification step, tissue sections were further processed for electron microscopic observation.

2.4. Electron Microscopy

Tissue processing for electron microscopy was done using modifications of published procedures (Chan et al., 1990, Pickel and Chan, 1993). Sections were rinsed in 0.1 M PB and incubated for 1 hour in 2% osmium tetroxide solution in 0.1 M PB on flat porcelain plate wells. After osmium processing, sections were dehydrated through a series of alcohol solutions and were then placed in propylene oxide. Sections were placed in vials containing equal parts of propylene oxide and Epon 812 mixture, and infiltrated overnight with gentle rotation at room temperature. Finally, sections were infiltrated with Epon 812 mixture for 2 hours with gentle rotation before flat-embedding between two sheets of plastic (Aclar, Ted Pella, Inc., Redding, CA). After polymerizing overnight in an oven at 65°C, plastic-embedded sections were examined with a stereomicroscope and small A5 cell group regions were roughly trimmed out and mounted on pre-formed resin blocks. Tissue sections that included noradrenergic neurons of both the rostral and caudal A5 cell group from two animals with BDA deposits in the ventrolateral PAG (Fig. 1) were selected for ultrastructural analysis. The rostrocaudal extend of the A5 cell group analysis corresponded to plates 56 to 62 of Paxinos' Atlas (Paxinos and Watson, 1997). Specifically, the rostral A5 sections were located at the level of the motor nucleus of the trigeminal nerve while the caudal sections were located at the level of the superior olive. Alternate 40 μm thick tissue sections were processed for either light or electron microscopic analysis. Since light microscopic analysis of anterogradely-labeled fibers was difficult in thick osmicated tissue sections, adjacent non-osmicated sections were viewed with a light microscope and camera lucida drawings were made (Fig. 2). We have used digital imaging software Neurolucida (MicroBrightField Inc., Colchester, VT) at different microscope objectives for creation of

camera lucida drawings. Neurolucida drawings containing outlines of coronal sections, anterogradely-labeled axons, and noradrenergic neurons were exported into the Corel Draw Graphic Suite using PC computer for final editing of presented schematic drawings. In contrast, the regions of interest (Fig. 2A and B) from thick osmicated tissue sections were affixed to an Epon Specimen block and viewed using a microscope equipped with a video camera. Visualization of the A5 cell group was used to guide the trimming of specimen blocks to include areas of tissue containing both BDA and TH immunolabeling. At least two 40 μm thick tissue sections per A5 subgroup from each brain were selected and 5-10 ultrathin sections approximately 80 nm thick were cut with a diamond knife (Diatome, Fort Washington, PA), placed on grids, and counterstained with 4% uranyl acetate and Reynold's lead citrate. Ultrathin sections were examined using a transmission electron microscope (JEOL 1220) and micrographs were prepared from regions of tissue located exclusively near the surface of the sections. All anterogradely-labeled profiles in the fields containing TH-ir profiles were examined and photographed at a magnification of x10,000. The photographic negatives were enlarged x2.5 for a final magnification of x25,000. The photomicrographs were examined and labeled profiles were classified. We did not digitally edit any of the presented photomicrographs (Figs. 3-5). This sample contained a total of 558 BDA-labeled profiles: 197 being anterogradely-labeled axon terminals, 273 BDA-labeled unmyelinated axons and 88 BDA-labeled myelinated axons (Table 1).

2.5. Data Analysis

2.5.1. Definition of cellular elements—Identification of cellular elements was based on the description of Peters et al. (Peters et al., 1991, Peters and Palay, 1996). Somata contained a nucleus, Golgi apparatus, smooth and granular endoplasmic reticulum. Proximal dendrites usually contained endoplasmic reticulum, Golgi apparatus, lysosomes and were larger than 5 μm in diameter. Dendrites with diameter greater than 2.5 μm usually exhibited only endoplasmic reticulum. Distal dendrites were postsynaptic to axon terminals and were approximately 0.5-2.0 μm in diameter. Axon terminals contained synaptic vesicles and were at least 0.3 μm in diameter. Being that individual profiles (e.g. terminal or dendrite) were rather elliptical instead of circular in shape, we measured two diameters (small and large) for each individual profile and presented it as separate values. Furthermore, a terminal was considered to form a synapse if it showed a junctional complex, a restricted zone of parallel membranes with slight enlargement of the intercellular space and/or associated postsynaptic thickening (Peters and Palay, 1996). Asymmetric synapses were identified by the presence of thick postsynaptic densities (Gray's Type I) (Gray, 1959), while symmetric synapses had thin densities (Gray's Type II) (Gray, 1959) located both pre- and post-synaptically. Non-synaptic contacts, or plasmalemmal appositions, were defined as cases in which the plasma membrane of an axon terminal was parallel to that of a dendrite, axon or soma, with no intervening glial processes, and no recognizable synaptic specializations.

2.5.2. Identification of silver-intensified gold labeling in profiles—Noradrenergic profiles were identified in single thin sections by the presence of at least 3 gold particles within a specific cytoplasmic compartment. Lightly labeled somatic and dendritic TH-ir profiles were confirmed by the presence of gold particles in at least two serial sections when possible. A profile containing a small number of gold particles (e.g. two gold particles) that was unlabeled in adjacent thin sections was designated as lacking detectable immunoreactivity. Because artifactual background labeling in the neuropil was not commonly encountered, the criterion of 3 gold particles as indicative of TH labeling is conservative and may have lead to an underestimation of the number of TH-labeled profiles. Another factor that may have contributed to an underestimation of labeled profiles is the limitation of immunocytochemical methods to detect trace amounts of TH. Finally, unbiased stereological methods were not used for counting labeled profiles and the results of the

numerical analysis can only be considered to be an estimate of the numbers of synapses and other labeled profiles.

3. RESULTS

3.1. Anterograde Tracer Deposits in the Ventrolateral Periaqueductal Gray

The anterograde tracer BDA was iontophoretically deposited into the ventrolateral division of the PAG of sixteen rats along its rostrocaudal axis. Previously published light microscopic analysis demonstrated identical pattern of labeling in all animals (Bajic and Proudfit, 1999). Figure 1 schematically illustrates representative location of BDA injection sites in the ventrolateral PAG of two cases that were selected for ultrastructural analysis of projections to the A5 cell group. Detailed drawings and photomicrographs of additional injection sites are shown in our previous reports (Bajic and Proudfit, 1999, Bajic et al., 2000, Bajic et al., 2001). The size of the effective tracer deposits was assumed to correspond to the dark ‘core’ area of the peroxidase reaction product, whereas the lighter ‘shaded’ area represents a dense concentration of BDA-labeled axons exiting from neurons at the injection site. Individual labeled neurons could often be detected in the zone of the injection site.

3.2. Light Microscopic Analysis of Anterogradely-Labeled Axons in the Rostral and Caudal Subdivisions of the A5 Cell Group

Noradrenergic neurons in he A5 cell group were identified by silver-intensified gold-labeling of antibodies directed against TH. This group of noradrenergic neurons consists of a cluster of large multipolar neurons in the area of the ventrolateral pons comprising the rostral subdivision of the A5 cell group (Fig. 2A), and a cluster in the ventrolateral rostral medulla comprising the caudal subdivision of the A5 cell group (Fig. 2B). BDA deposits in the ventrolateral PAG (Fig. 1) produced moderately dense anterograde labeling of axons in the ipsilateral region of the A5 cell group (Fig. 2C and D) in all sixteen cases examined, but fewer labeled axons were found in the area of the A5 cell group on the contralateral side (not shown). The medial two thirds of the rostral A5 and the medial half of the caudal A5 cell group (Fig. 2C and D) contained a dense plexus of varicose processes resembling a terminal field i.e. they contained branching axons that ended in terminal boutons and many axons exhibited numerous varicosities that may represent en passant synapses. Peroxidase-labeled axon terminals with *en passant* or terminal varicosities were often seen apposed to TH-ir dendrites, but were only rarely seen apposed to TH-ir somata. Many anterogradely-labeled axons appeared to target non-catecholamine neurons. In contrast, the lateral third of the A5 cell group of both subdivisions was largely devoid of labeled axons.

3.3. Ultrastructural Analysis of Anterogradely-Labeled Axons in the A5 Cell Group

3.3.1. Characteristics of biotinylated dextran amine-labeled profiles—

Anterograde labeling of the BDA was identified in all samples that included the neuropil of either the rostral or caudal subdivisions of the A5 cell group (Fig. 2A and B). The anterogradely transported BDA label was identified in both myelinated and unmyelinated axons (Fig. 3A and 4B) and in synaptic terminals (Figs. 3-5) in the area of the A5 cell group. Estimated frequency of BDA-labeled profiles identified in both rostral and caudal subdivisions of the A5 cell group is represented in Table 1. The mean small diameter of all identified BDA-labeled terminals in the A5 cell group was 0.8 ± 0.03 μm and the mean large diameter was 1.43 ± 0.1 μm and the distribution of diameters was approximately normal with a range of 0.2 – 3.61 μm (n=197; Table 2). The appearance of peroxidase reaction product in BDA-labeled terminals differed depending on the intensity of labeling. Specifically, 60% (76/127) of the anterogradely-labeled terminals in the rostral A5, and about 53% (37/70) in the caudal A5 were intensely labeled. These terminals contained dense flocculent precipitate that often obscured the clear identification of vesicle morphology and

synaptic specializations (Fig. 5A). In contrast, the remaining 40% (51/127) in the rostral A5 and about 47% (33/70) in the caudal A5 were lightly to moderately labeled terminals. These terminals contained dark-rimmed vesicles and a light to moderate amount of dense flocculent label that allowed unequivocal identification of vesicle morphology and synaptic specializations (Figs. 3, 4, and 5B). All of the identified lightly anterogradely-labeled terminals contained densely packed small round clear vesicles (Figs. 4 and 5B) with a mean diameter of 35 nm. Furthermore, about 31% (16/51) in the rostral A5 and about 30% (10/33) in the caudal A5 of those lightly labeled BDA terminals, in addition to small round clear vesicles, also contained a few large dense-core vesicles with diameters of 70-100 nm that were usually located near the plasma membrane but away from synaptic specializations (Figs. 4 and 5B).

In addition, the mean small diameter of BDA-labeled terminals that formed synapses with, or had plasmalemmal appositions to unlabeled dendrites was 0.81 ± 0.03 μm and the mean large diameter was 1.37 ± 0.05 μm and the distribution of diameter was approximately normal with a range of 0.2 – 3.61 μm (n=121; Table 2). Similarly, the mean small diameter of BDA-labeled terminals that formed synapses with, or had plasmalemmal appositions to TH-ir dendrites was 0.81 ± 0.07 μm and the mean large diameter was 1.38 ± 0.09 μm and the distribution of these terminal diameters was also approximately normal with a range of 0.22 – 2.22 μm (n=25; Table 2). Finally, BDA-labeled terminals that formed appositions to unlabeled terminals (n=133; Table 2) had a mean small diameter of 0.81 ± 0.04 μm (n= 65) and the mean large diameter was 1.27 ± 0.06 μm (n=68) with approximately normal distribution with a range of 0.3 – 2.35 μm. Finally, only 1 and 3 retrogradely-labeled dendrites were found at the electron microscopic levels of resolution in the rostral and caudal A5 cell groups, respectively (not shown).

3.3.2. Characteristics of tyrosine hydroxylase-immunoreactive profiles in the A5 cell group—Dense flocculent peroxidase labeling of BDA profiles was clearly distinguishable from the TH-ir silver-enhanced immunogold labeling that appeared as black irregular round or rod-shaped particles within catecholamine profiles in the A5 cell group. The immunogold labeling that was uniformly distributed in a dendritic (Fig. 4), somatic cytoplasm, and occasionally in catecholamine axons and terminals did not appear to be either segregated or associated with any particular organelle. Numerous organelles, such as rough endoplasmic reticulum, Golgi apparatus, lysosomes and mitochondria, were present in the cytoplasm of labeled proximal dendrites (Fig. 4A), whereas nuclei were only clearly visible in cross sections of the TH-ir perikarya. Distal dendrites contained only mitochondria (Fig. 4B and C). Astrocytic processes covered most of the perikaryal plasmalemma of the noradrenergic neurons in the A5 cell group, while noradrenergic somata received sparse synaptic input from unlabeled axon terminals filled with small clear vesicles (not shown). Noradrenergic somata of the A5 cell group were approximately 35 – 50 μm in diameter, whereas the labeled large proximal dendrites were about 9 – 10 μm in diameter.

Most of the BDA-labeled terminals formed appositions or synapses with small to medium TH-ir dendrites; these dendrites had a mean small diameter of 1.31 ± 0.14 μm and mean large diameter of 3.24 ± 0.28 μm and fell within the range of 0.55 – 5.55 μm (n=20). Only five TH-ir proximal dendrites, with mean small diameter of 4.65 ± 1.37 μm and mean large diameter of 5.83 ± 0.9 μm, were identified to form synapses with BDA-labeled terminals. These TH-ir proximal dendrites fell within the range of 2.33 to more than 8 μm. Similarly, the majority of BDA-labeled terminals also formed appositions or synapses with small to medium unlabeled dendrites; these dendrites had a mean small diameter of 1.06 ± 0.06 μm and mean large diameter of 2.05 ± 0.13 μm and fell within the range of 0.26 – 5.47 μm (n=117). Only four unlabeled proximal dendrites, with mean small diameter of 1.84 ± 0.2 μm and mean large diameter of 5.49 ± 0.55 μm were identified to form synapses with BDA-

labeled terminals. Note that distribution of both labeled and unlabeled dendrites were skewed towards the smaller diameters and had median diameter in the range of the 1.19 – 2.97 μm and 0.99 – 1.77 μm, respectively. Finally, unlabeled terminals that formed appositions or synapses with BDA-labeled terminals in the region of the A5 cell group had a mean small diameter of 0.83 ± 0.05 μm and mean large diameter of 1.32 ± 0.05 μm and had a median diameter in the range of 0.71 – 1.28 μm. The distribution of unlabeled terminals was approximately normal in the range of 0.17 – 2.27 μm (n=133; Table 2). Size characteristics of unlabeled terminals were very similar to those of BDA-labeled terminals with which they made synapses (Fig. 5).

3.3.3. Characteristics of synapses formed by biotinylated dextran amine-labeled terminals—Figure 2A and B illustrates areas of the ventrolateral pons comprising the rostral and caudal subdivision of the A5 cell group, respectively, that were sampled for the ultrastructural analysis. As suggested by light microscopic analysis, the density of anterogradely-labeled axons in the rostral subdivision of the A5 cell group was greater than that in the caudal A5 subdivision. This observation was confirmed at the ultrastructural level by differences between the numbers of BDA-labeled profiles identified in samples from the rostral vs. caudal A5 subgroups (Table 1). Specifically, a total of 127 BDA-labeled terminals were identified in the rostral A5 cell group, and only 70 were identified in the caudal A5 cell group. Furthermore, a total of 293 plasmalemmal appositions and synapses (Table 2) formed by total of 197 BDA-labeled terminals (Table 1) were identified in samples from the rostral and caudal subdivisions of the A5 cell group. Thus, almost 50% of the anterogradely-labeled terminals exhibited membrane appositions to, or formed synapses with, two or more postsynaptic profiles.

3.3.4. Projection of ventrolateral PAG neurons to the rostral A5 cell group—As shown in Table 2, in the rostral subdivision of the A5 cell group, approximately 43% (86/201) of appositions or synapses were formed by BDA-labeled terminals with unlabeled dendrites, whereas about 8% (16/201) were formed with TH-ir dendrites (Fig. 4A,C and D). In addition, only a few synapses or plasmalemmal appositions were associated with unlabeled axons (Fig. 3C) and about 45% (90/201) were made with unlabeled axon terminals (Fig. 5). Although the latter appeared to be axo-axonic synapses, the density of the labeling prevented clear identification of synaptic specializations in most of the cases. Nearly all of the unlabeled terminals, that were postsynaptic to BDA-labeled terminals, formed synapses with unlabeled dendrites (Fig. 5), but only rarely with TH-ir dendrites (not shown) in the neuropil of the rostral A5 cell group. Only 4% (9/201) of apposition were formed with dendrites that could not be unambiguously identified as containing TH-ir. Finally, a total of 127 BDA-labeled terminals (Table 1) formed a total of 201 contacts (synapses or plasmalemmal appositions; Table 2) with profiles such as TH-ir dendrites, unlabeled dendrites, or unlabeled terminals, and approximately 75% (96/127) of these were also closely apposed to surrounding astrocytic processes (Figs. 3, 4C,D and 5). The cytoplasm of the astrocytic processes contained few organelles and sometimes appeared largely empty, presumably due to their known tendency to swell in fixed tissues (Peters et al., 1991). The BDA-labeled terminals from neurons in the ventrolateral PAG often contained dense peroxidase reaction product that prevented clear identification of synaptic types. However, about 33% (28/86) of all the BDA-labeled terminals in the sample from the rostral A5 formed clearly recognizable synaptic specializations with unlabeled postsynaptic profiles (Table 3). When synapses formed by BDA-labeled terminals with unlabeled profiles were clearly identifiable, 21% (18/86) were symmetric (Gray's Type II) synapses and 12% (10/86) were asymmetric (Gray's Type I) synapses (Fig. 3B and C). About 67% (58/86) of the BDA-labeled terminals exhibited plasmalemmal apposition to unlabeled neuronal profiles, but lacked clear synaptic specializations. Similarly, when synapses formed by

BDA-labeled terminals with TH-ir dendrites in the rostral A5 cell group were clearly identifiable, 31% (5/16) were symmetric (Gray's Type II) synapses (Fig. 4A) and 19% (3/16) were asymmetric (Gray's Type I) synapses (Fig.4C). Finally, about 50% (8/16) of the BDA terminals that exhibited plasmalemmal appositions to TH-ir dendritic profiles did not exhibit clear synaptic specializations in the planes of section analyzed. These characteristics of BDA-labeled synaptic terminals are summarized in Table 3.

3.3.5. Projection of ventrolateral PAG neurons to the caudal A5 cell group—

The neuropil of the ipsilateral caudal A5 cell group contained a dense concentration of TH-ir perikarya and dendrites but a much lower density of anterogradely-labeled profiles than that in the rostral A5 cell group (Fig. 2; Table 1). Since single BDA-labeled terminals formed contacts with more than one postsynaptic profile, a total of 92 appositions and synapses (Table 2) formed by 70 BDA-labeled terminals (Table 1) were identified in the caudal A5 cell group. More specifically, about 38% (35/92) of BDA-labeled terminals formed synapses with unlabeled dendrites, whereas 10% (9/92) formed synapses with TH-ir dendrites (Fig. 4B). In addition, only a few synapses or plasmalemmal appositions were associated with unlabeled axons (Fig. 3A) and about 47% (43/92) were made with unlabeled axon terminals (Fig. 5D). Similar to the rostral A5 cell group, no anterogradely-labeled terminals formed synapses with either noradrenergic or non-catecholaminergic somata in the caudal A5 cell group. Only 5% (5/92) of the BDA-labeled terminals formed synapses with dendrites that could not be unambiguously defined as containing TH-ir (Table 2). Finally, approximately 78% (55/70) of all identified BDA-labeled terminals were also closely apposed to surrounding astrocytic processes in the caudal A5 cell group (Figs. 3A and 5D).

Anterogradely-labeled terminals in the caudal A5 cell group often contained dense peroxidase reaction product that prevented clear identification of synaptic types. When synapses formed by BDA-labeled terminals and unlabeled dendrites were clearly identifiable, 31% (11/35) were symmetric (Gray's Type II) synapses, whereas the remaining 69% (24/35) of the BDA terminals that were closely apposed to unlabeled dendrites did not exhibit clear synaptic specializations in the planes of section analyzed but did not have intervening astrocytic processes. Similarly, for cases in which labeled terminals and TH-ir dendrites were closely apposed, but did not have intervening astrocytic processes, 22% (2/9) formed clearly identifiable symmetric (Gray's Type II) synapses, and about 78% (7/9) did not exhibit clear synaptic specializations in the planes of section analyzed. Note that no asymmetric synapses were identified between BDA-labeled terminals originating from the ventrolateral PAG and either unlabeled or TH-ir profiles in the caudal A5 cell group. These characteristics of BDA-labeled synaptic terminals are summarized in Table 3.

4. DISCUSSION

The results from this study provide the first ultrastructural evidence from dually labeled sections that BDA-labeled axon terminals originating from neurons in the ventrolateral PAG form (1) symmetric and asymmetric synapses with unlabeled and TH-ir dendrites, and (2) may presynaptically modulate local interneurons or afferents to the A5 cell group region from other brain areas.

4.1. Methodological Considerations

Electron microscopic determination of synapses based on combined anterograde transport and immunocytochemical detection of an antibody has several limitations. The main problem is related to limited and/or differential penetration of primary and secondary antisera in 40 μm-thick tissue sections. Limited penetration of the TH antiserum may have contributed to an underestimation of the relative frequencies of synapses found on TH-ir dendrites in the brain regions sampled. This potential limitation was minimized by collecting

sections near the tissue surface and by ensuring that both labels were clearly present in fields included for analysis. Another factor that might have contributed to an underestimation of the relative frequencies of synapse types was that the BDA reaction product often obscured the morphological detail of both the labeled terminals and the presynaptic specializations. Other limitations are inherent in all transport studies, and these include the spread of anterograde tracer from the injection site, uptake by neurons in neighboring brain areas and retrograde labeling of neurons that project to the tracer injection site (Wouterlood and Jorritsma-Byham, 1993). In this study, the BDA deposits were confined to the ventrolateral PAG and did not spread to the surrounding regions. In addition, the distribution of BDA-labeled axons and terminals within the pons was comparable to that of Phaseolus vulgaris-leucoagglutining (PHA-L), another anterograde tracer with different structural and transport characteristics (Gerfen et al., 1989, Wouterlood and Jorritsma-Byham, 1993, Dolleman-Van der Weel et al., 1994). In addition, we have previously demonstrated identical monosynaptic projections of neurons in the ventrolateral PAG both to the locus coeruleus (A6) (Bajic et al., 2000) and the A7 noradrenergic cell groups (Bajic et al., 2001) using either the BDA or PHA-L. Similarly, virtually identical labeling patterns were reported when using either PHA-L (Clark and Proudfit, 1991c) or BDA (Holden and Proudfit, 1998) to determine the efferent projections of neurons in the ventromedial medulla. Finally, only a few retrogradely-labeled neurons were found in samples from the A5 cell group, and it is unlikely that these contributed a significant amount of labeling.

4.2. Ventrolateral PAG Projections to the A5 Cell Group

4.2.1. Monosynaptic pathway—Our previous light microscopic study (Bajic and Proudfit, 1999) provided presumptive evidence for a direct pathway from neurons in the ventrolateral PAG to the noradrenergic neurons in the A5 cell group. The results of the present study confirm those findings, but also provide unequivocal direct ultrastructural evidence for a monosynaptic pathway from ventrolateral PAG neurons to both noradrenergic and non-catecholaminergic neurons in the region of noradrenergic A5 cell group. Density of labeled axons in the rostral A5 cell group is significant, whereas the caudal A5 contains fewer labeled axons. In contrast, study by Cameron et al. (Cameron et al., 1995), which used PHA-L for anterograde tracer, rather than BDA, did not observe such a pathway from the ventrolateral PAG to the region of the A5 cell group. These researchers reported only sparse PHA-L-labeled axons in the A5 cell group after tracer injections into either the rostral or caudal parts of the ventrolateral PAG. In accordance with characteristics and projection similarities of two different tracers used, as mentioned above, it is difficult to explain different findings only on the basis of methodological differences. It is also possible that the reported differences in the projections of PAG neurons to the region of the noradrenergic A5 cell group reflect differences in neuronal circuitry. In fact, we have previously reported fundamental differences in the projections of noradrenergic neurons to the spinal cord (Clark and Proudfit, 1991a, Clark et al., 1991, Proudfit and Clark, 1991, Clark and Proudfit, 1992, Proudfit, 2002), and demonstrated differences in the physiological function of these neurons in different outbred stocks of Sprague-Dawley rats (West et al., 1993, Graham et al., 1997).

4.2.2. Postsynaptic excitation—Minor direct monosynaptic projections from the ventrolateral PAG to the rostral subdivision of the A5 cell group may produce excitation of A5 neurons. Ultrastructural analysis provides evidence to suggest that some synapses formed by PAG efferents with noradrenergic and non-catecholaminergic dendrites in the rostral A5 cell group may contain excitatory neurotransmitters. Of all identified plasmalemmal contacts of anterogradely-labeled terminals in the rostral A5 cell group, 19% (3/16) formed asymmetric synapses with TH-ir profiles and about 12% (10/86) with unlabeled dendrites (Table 3). Asymmetric (Gray's Type I) synapses have been correlated with excitatory transmission and often contain transmitters with excitatory actions such as

glutamate (Peters et al., 1991) or substance P (Pickel et al., 1979, Milner and Pickel, 1986, Proudfit and Monsen, 1999). Although there are neurons in the ventrolateral PAG that contain both glutamate (Beitz, 1990) and substance P (Hokfelt et al., 1977b, Ljungdahl et al., 1978b, Hokfelt et al., 1979, Shults et al., 1984, Smith et al., 1994), there is no anatomical evidence that those neurons project to the area of the A5 cell group. There is only evidence that axon terminals containing either glutamate (Helfert et al., 1992) or substance P (Ljungdahl et al., 1978a, Ljungdahl et al., 1978b, Shults et al., 1984) are present in the region of the A5 cell group and that the substance P receptors are located on the noradrenergic dendrites of the A5 neurons (D. Bajic and H.K. Proudfit, unpublished observations). Since no asymmetric synapses were identified in the caudal A5 cell group, our findings suggest that excitatory neurons in the ventrolateral PAG might project to and activate neurons only in the rostral A5 cell group. However, these direct excitatory afferents constitute a minor fraction of identified ventrolateral PAG projections to the A5 cell group.

4.2.3. Postsynaptic inhibition—In contrast to the excitatory effects on the noradrenergic neurons of the A5 cell group, it is possible that another population of neurons in the ventrolateral PAG may have an inhibitory effect on either local interneurons or projection neurons in the region of both the rostral and the caudal A5 cell group. Specifically, about 43% of the identified anterogradely-labeled terminals contained small (20-30 nm) clear vesicles that are known to contain the inhibitory neurotransmitter GABA (Reichling and Basbaum, 1990, Peters et al., 1991, Kwiat et al., 1993, Peters and Palay, 1996, Skinner et al., 1997, Van Bockstaele and Chan, 1997). In addition, about 31% of these also contained large (70-100 nm) dense-core vesicles that are known to contain neuropeptides, such as the inhibitory neurotransmitter enkephalin (Pickel et al., 1979, Peters et al., 1991, Commons and Milner, 1996, Van Bockstaele et al., 1996). Furthermore, the majority of clearly identified synapses formed by BDA-labeled terminals with unlabeled dendrites (24%) and noradrenergic dendrites (28%) in the A5 cell group were symmetric (Gray's Type II) synapses (Table 3) that have been correlated with inhibitory neurotransmission and often contain GABA (Ribak et al., 1981, Pickel et al., 1988, Reichling and Basbaum, 1990, Cho and Basbaum, 1991, Peters et al., 1991, Van Bockstaele and Chan, 1997) or enkephalin (Van Bockstaele et al., 1995, Commons and Milner, 1996, Van Bockstaele et al., 1996). Both GABA (Mugnaini and Oertel, 1985, Reichling and Basbaum, 1990) and enkephalin (Hokfelt et al., 1977a, Petrusz et al., 1985, Smith et al., 1994) are present in the neurons of the ventrolateral PAG. Although many GABA neurons project beyond the borders of the PAG (Reichling and Basbaum, 1990), and terminals containing GABA (Kwiat et al., 1993) or enkephalin (Pickel et al., 1979) (D. Bajic and H.K. Proudfit, unpublished observations) are present in the region of the A5 cell group, there is no direct anatomical evidence that either GABA or enkephalin neurons in the ventrolateral PAG project to the region of the A5 cell group. Moreover, functional data supporting these observations are lacking. Therefore, additional studies are needed to provide definitive evidence that either GABA or enkephalin neurons in the ventrolateral PAG project to and inhibit neurons of the A5 cell group. This pathway may ultimately lead to disinhibition of spinally-projecting noradrenergic neurons of the A5 cell group. Anatomical evidence indicates that some of these non-catecholamine neurons may contain GABA (Mugnaini and Oertel, 1985), however, whether they may represent local interneurons tonically inhibiting spinally-projecting noradrenergic A5 neurons remains to be investigated.

4.2.4. Presynaptic inhibition—In addition to direct postsynaptic inhibition or excitation by PAG afferents to the A5 cell group, PAG neurons may also presynaptically influence synaptic transmission in the A5 cell group. In both rostral and caudal A5 cell group, about 45% and 47% respectively, of all the appositions made by anterogradely-labeled axon terminals had direct plasma membrane appositions to other unlabeled axon terminals that

formed synapses with mostly non-catecholaminergic dendrites, and only sparsely to TH-ir dendrites. Described axoaxonic arrangement indicates that almost half of the neurons in the ventrolateral PAG that project to the A5 cell group modulate the terminal excitability of other afferent projections, or local circuit neurons in the region of the A5 cell group. Future anatomical and functional studies should elucidate influence of inhibitory and/or excitatory axoaxonic cross talk from ventrolateral PAG on A5 cell group output.

4.3. Functional Implications

It is well established that ventrolateral PAG is an important brainstem site whose activation throughout the rostrocaudal axis of the ventrolateral PAG produces a syndrome designated as *hyporeactive immobility* (Bandler and Depaulis, 1991), which is characterized by cessation of locomotion, decreased spontaneous behaviors, decreased responses to external stimuli, potent antinociception as well as sympathoinhibition of cardiovascular reflexes (Lovick, 1991, Jones, 1992, Bandler and Shipley, 1994, Dean, 2005). Previous anatomical studies have demonstrated that noradrenergic neurons in the A5 cell group innervate the intermediolateral cell column in thoracic spinal cord segments (Loewy et al., 1979, Byrum and Guyenet, 1987, Romagnano et al., 1991, Clark and Proudfit, 1993), as well as spinal cord laminae IV-VII (Clark and Proudfit, 1993), where numerous nociceptive neurons are located (Light, 1992). Recent study by Bruinstroop et al. (Bruinstroop et al., 2012), which used novel genetically specified viral vector-based tracing method for noradrenergic neurons, showed that the A5 cell group supplies only sparse innervation to the dorsal horn, but provides the densest innervation to the thoracic intermediolateral cell column, and in particular to the sympathetic preganglionic neurons. Thus, the A5 cell group may be a primary mediator of sympathoinhibition and, to a lesser extent, a mediator of antinociception.

4.3.1. Modulation of cardiovascular reflexes—It was demonstrated that stimulation of neurons in the ventrolateral PAG elicited by microinjection of excitatory amino acids produces a prominent cardiovascular depressor response, characterized by an abrupt fall in arterial pressure and a substantial bradycardia (Bandler and Depaulis, 1991, Carrive and Bandler, 1991, Lovick, 1992, Bandler and Shipley, 1994, Keay et al., 1997). Anatomical basis of this sympathoinhibition implicates significant projections of neurons from the ventrolateral PAG to two major vasodepressor regions: the caudal ventrolateral medulla (CVLM) and the caudal midline medulla (CMM) (Henderson et al., 1998). It was proposed that sympathoinhibition produced by stimulation of the ventrolateral PAG may be mediated in part by neurons in the CMM, which includes the nucleus raphe magnus, as well as neurons in the CVLM that inhibit sympathoexcitatory neurons in the vasopressor regions of the rostral ventrolateral medulla (RVLM) (Benarroch et al., 1986, Granata et al., 1986, Lovick, 1993, Jeske et al., 1995, Henderson et al., 1998). In addition to projecting to the RVLM (Holtman et al., 1990, Ellenberger and Feldman, 1994, Holtman and Speck, 1994, Zagon, 1995), the CMM also innervates sympathetic preganglionic neurons in the intermediolateral cell column of the spinal cord (Loewy, 1981, Bacon et al., 1990, Aicher et al., 1994, Allen and Cechetto, 1994, Aicher et al., 1995, Jansen et al., 1995). The functional significance of the latter pathway is supported by studies, which have demonstrated that injection of 5-hydroxytryptamine antagonists into the intermediolateral column attenuates sympathoinhibition evoked by electrical stimulation in the region of the raphe nuclei including the CMM (Gilbey et al., 1981). In addition to the proposed spinally-projecting serotonergic pathway in mediating sympathoinhibition, the A5 cell group was also implicated in hemodynamic control. Neurons of the A5 group innervate the intermediolateral cell column (Loewy et al., 1979, Byrum and Guyenet, 1987, Romagnano et al., 1991, Clark and Proudfit, 1993, Bruinstroop et al., 2012), while stimulation of A5 neurons with microinjection of glutamate produces a depressor effect (Stanek et al., 1984,

Burnett and Gebhart, 1991). Reported pressor effect produced by electrical stimulation of sites near A5 neurons (Loewy et al., 1986, Drye et al., 1990) resulted from activation of fibers of passage. Finally, microelectrophoretically applied noradrenaline inhibits single sympathetic preganglionic neurons in the thoracic segment of the spinal cord activated by electrical stimulation of a brainstem excitatory region (Coote et al., 1981). However, we demonstrated very few monosynaptic projections with asymmetric synapses on noradrenergic neurons in the rostral, and none in the caudal A5 cell group (Table 3). Thus, it is unlikely that the ventrolateral PAG cardiovascular responses are mediated primarily via direct excitatory relay at the A5 cell group. Considering that the majority of BDA-labeled terminals originating from ventrolateral PAG formed symmetric synapses and almost 50% formed axoaxonic contacts in the A5 cell group, future studies should further elucidate complex anatomical and functional interplay of ventrolateral PAG projections to the A5 cell group (e.g. disinhibition of spinally projecting noradrenergic neurons of the A5 cell group).

4.3.2. Modulation of nociception—Both electrical (Fang and Proudfit, 1996, 1998) and chemical (Yaksh, 1979, Jensen and Yaksh, 1984, 1986) stimulation of ventrolateral PAG neurons produces antinociception that can be blocked by intrathecal a-adrenoceptor antagonists, suggesting that antinociception produced by activating neurons in the ventrolateral PAG is mediated in part by spinally-projecting noradrenergic neurons. Previous anatomical (Bajic and Proudfit, 1999, Bajic et al., 2001) and pharmacological (Yeomans et al., 1992, Yeomans and Proudfit, 1992, Holden et al., 1999) studies have implicated noradrenergic neurons in the A7 cell group as the most likely neurons of the brainstem catecholaminergic groups to mediate the antinociception produced by stimulation of sites in the ventrolateral PAG because A7 neurons project to the superficial laminae of the rat spinal cord dorsal horn (Clark and Proudfit, 1991b), where numerous nociceptive neurons are located (Light, 1992). Similarly, neurons located in the A5 cell group in Sasco Sprague-Dawley rats innervate the spinal cord dorsal horn (Clark and Proudfit, 1993, Bruinstroop et al., 2012), while both electrical (Miller and Proudfit, 1990) and chemical (Burnett and Gebhart, 1991) stimulation of sites near the A5 cell group can produce antinociception that is reduced by intrathecal injection of alpha$_2$-adrenoceptor antagonists. However, considering a minor monosynaptic projection from ventrolateral PAG with asymmetric synapses on noradrenergic neurons in the rostral, and none in the caudal A5 cell group (Table 3), it is unlikely that the established monosynaptic pathway plays a significant role in the ventrolateral PAG antinociceptive effects. Future studies are needed to evaluate the role of the noradrenergic neurons of the A5 cell group as a possible, indirect relay for the ventrolateral PAG antinociceptive effects.

5. CONCLUSIONS

The results of this study provide direct ultrastructural evidence that neurons in the ventrolateral PAG form synapses with the dendrites of noradrenergic as well as non-catecholaminergic neurons of the A5 cell group. Future studies should reveal if the latter are projection neurons or local interneurons of the A5 cell group. Furthermore, the finding of axoaxonic synapses supports the hypothesis that neurons in the ventrolateral PAG also influence the synaptic transmission of other afferent projections to dendrites of A5 neurons. The majority of axonal terminals originating from the ventrolateral PAG formed symmetric synapses on non-catecholaminergic neurons in both the rostral and caudal A5 cell group. In contrast, we identified very few monosynaptic projections with asymmetric synapses on noradrenergic neurons in rostral, and none in the caudal A5 cell group, suggesting that the A5 cell group does not represent a direct relay for sympathoinhibition and antinociception elicited by stimulation of ventrolateral PAG. Additional studies utilizing this data should correlate the physiological responses of individual subclasses of A5 neurons with their morphology and synaptic inputs from neurons originating in the ventrolateral PAG.

Acknowledgments

This work was supported by USPHS grant DAO3980 from the National Institutes on Drug Abuse to H.K. Proudfit and grants ANA#96002249 and NIDA 09082 to E.J. Van Bockstaele.

ABBREVIATIONS

BDA	biotinylated dextran amine
BSA	bovine serum albumin
CMM	central medial medulla
CVLM	caudal ventrolateral medulla
GAD	glutamate decarboxylase
PAG	periaqueductal gray
PB	phosphate buffer
PBS	phosphate buffered saline
PHA-L	*Phaseolus vulgaris* leucoagglutinin
RVLM	rostral ventrolateral medulla
TBS	Tris-buffered saline
TH	tyrosine hydroxylase
TH-ir	tyrosine hydroxylase-immunoreactivity

LITERATURE CITED

Aicher SA, Reis DJ, Nicolae R, Milner TA. Monosynaptic projections from the medullary gigantocellular reticular formation to sympathetic preganglionic neurons in the thoracic spinal cord. J Comp Neurol. 1995; 363:563–580. [PubMed: 8847418]

Aicher SA, Reis DJ, Ruggiero DA, Milner TA. Anatomical characterization of a novel reticulospinal vasodepressor area in the rat medulla oblongata. Neuroscience. 1994; 60:761–779. [PubMed: 7936200]

Allen GV, Cechetto DF. Serotoninergic and nonserotoninergic neurons in the medullary raphe system have axon collateral projections to autonomic and somatic cell groups in the medulla and spinal cord. J Comp Neurol. 1994; 350:357–366. [PubMed: 7533797]

Bacon SJ, Zagon A, Smith AD. Electron microscopic evidence of a monosynaptic pathway between cells in the caudal raphe nuclei and sympathetic preganglionic neurons in the rat spinal cord. Exp Brain Res. 1990; 79:589–602. [PubMed: 2340876]

Bajic D, Proudfit HK. Projections of neurons in the periaqueductal gray to pontine and medullary catecholamine cell groups involved in the modulation of nociception. J Comp Neurol. 1999; 405:359–379. [PubMed: 10076931]

Bajic D, Proudfit HK, Van Bockstaele EJ. Periaqueductal gray neurons monosynaptically innervate extranuclear noradrenergic dendrites in the rat pericoerulear region. J Comp Neurol. 2000; 427:649–662. [PubMed: 11056470]

Bajic D, Van Bockstaele EJ, Proudfit HK. Ultrastructural analysis of ventrolateral periaqueductal gray projections to the A7 catecholamine cell group. Neuroscience. 2001; 104:181–197. [PubMed: 11311541]

Bandler, R.; Carrive, P.; Depaulis, A. Emerging prin ciples of organization of the midbrain periaqueductal gray matter. In: Depaulis, A.; Bandler, R., editors. The Midbrain Periaqueductal Gray Matter. Plenum; New York: 1991. p. 1-8.

Bandler, R.; Depaulis, A. Midbrain periaqueductal gray control of defensive behavior in the cat and rat. In: Depaulis, A.; Bandler, R., editors. The Midbrain Periaqueductal Gray Matter. Plenum; New York: 1991. p. 175-198.

Bandler R, Shipley MT. Columnar organization in the midbrain periaqueductal gray: modules for emotional expression? Trends Neurosci. 1994; 17:379–389. [PubMed: 7817403]

Beitz AJ. Relationship of glutamate and aspartate to the periaqueductal gray-raphe magnus projection: analysis using immunocytochemistry and microdialysis. J Histochem Cytochem. 1990; 38:1755–1765. [PubMed: 1701457]

Benarroch EE, Granata AR, Ruggiero DA, Park DH, Reis DJ. Neurons of C1 area mediate cardiovascular responses initiated from ventral medullary surface. Am J Physiol. 1986; 250:R932–945. [PubMed: 2871767]

Bruinstroop E, Cano G, Vanderhorst VG, Cavalcante JC, Wirth J, Sena-Esteves M, Saper CB. Spinal projections of the A5, A6 (locus coeruleus), and A7 noradrenergic cell groups in rats. J Comp Neurol. 2012; 520:1985–2001. [PubMed: 22173709]

Burnett A, Gebhart GF. Characterization of descending modulation of nociception from the A5 cell group. Brain Res. 1991; 546:271–281. [PubMed: 1676926]

Byrum CE, Guyenet PG. Afferent and efferent connections of the A5 noradrenergic cell group in the rat. J Comp Neurol. 1987; 261:529–542. [PubMed: 2440916]

Cameron AA, Khan IA, Westlund KN, Willis WD. The efferent projections of the periaqueductal gray in the rat: a Phaseolus vulgaris-leucoagglutinin study. II. Descending projections. J Comp Neurol. 1995; 351:585–601. [PubMed: 7721985]

Carrive P, Bandler R. Viscerotopic organization of neurons subserving hypotensive reactions within the midbrain periaqueductal grey: a correlative functional and anatomical study. Brain Res. 1991; 541:206–215. [PubMed: 2054638]

Chan J, Aoki C, Pickel VM. Optimization of differential immunogold-silver and peroxidase labeling with maintenance of ultrastructure in brain sections before plastic embedding. J Neurosci Methods. 1990; 33:113–127. [PubMed: 1977960]

Cho HJ, Basbaum AI. GABAergic circuitry in the rostral ventral medulla of the rat and its relationship to descending antinociceptive controls. J Comp Neurol. 1991; 303:316–328. [PubMed: 2013643]

Clark FM, Proudfit HK. The projection of locus coeruleus neurons to the spinal cord in the rat determined by anterograde tracing combined with immunocytochemistry. Brain Res. 1991a; 538:231–245. [PubMed: 2012966]

Clark FM, Proudfit HK. The projection of noradrenergic neurons in the A7 catecholamine cell group to the spinal cord in the rat demonstrated by anterograde tracing combined with immunocytochemistry. Brain Res. 1991b; 547:279–288. [PubMed: 1884202]

Clark FM, Proudfit HK. Projections of neurons in the ventromedial medulla to pontine catecholamine cell groups involved in the modulation of nociception. Brain Res. 1991c; 540:105–115. [PubMed: 1711394]

Clark FM, Proudfit HK. Anatomical evidence for genetic differences in the innervation of the rat spinal cord by noradrenergic locus coeruleus neurons. Brain Res. 1992; 591:44–53. [PubMed: 1446232]

Clark FM, Proudfit HK. The projections of noradrenergic neurons in the A5 catecholamine cell group to the spinal cord in the rat: anatomical evidence that A5 neurons modulate nociception. Brain Res. 1993; 616:200–210. [PubMed: 7689410]

Clark FM, Yeomans DC, Proudfit HK. The noradrenergic innervation of the spinal cord: differences between two substrains of Sprague-Dawley rats determined using retrograde tracers combined with immunocytochemistry. Neurosci Lett. 1991; 125:155–158. [PubMed: 1715531]

Clement CI, Keay KA, Owler BK, Bandler R. Common patterns of increased and decreased fos expression in midbrain and pons evoked by noxious deep somatic and noxious visceral manipulations in the rat. J Comp Neurol. 1996; 366:495–515. [PubMed: 8907361]

Clement CI, Keay KA, Podzebenko K, Gordon BD, Bandler R. Spinal sources of noxious visceral and noxious deep somatic afferent drive onto the ventrolateral periaqueductal gray of the rat. J Comp Neurol. 2000; 425:323–344. [PubMed: 10972936]

Commons KG, Milner TA. Ultrastructural relationships between leu-enkephalin- and GABA-containing neurons differ within the hippocampal formation. Brain Res. 1996; 724:1–15. [PubMed: 8816250]

Coote JH, Macleod VH, Fleetwood-Walker S, Gilbey MP. The response of individual sympathetic preganglionic neurones to microelectrophoretically applied endogenous monoamines. Brain Res. 1981; 215:135–145. [PubMed: 7260583]

Dahlstroem A, Fuxe K. Evidence for the Existence of Monoamine-Containing Neurons in the Central Nervous System. I. Demonstration of Monoamines in the Cell Bodies of Brain Stem Neurons. Acta Physiol Scand Suppl SUPPL. 1964; 232:231–255.

Dean C. Sympathoinhibition from ventrolateral periaqueductal gray mediated by the caudal midline medulla. Am J Physiol Regul Integr Comp Physiol. 2005; 289:R1477–1481. [PubMed: 16221983]

Dolleman-Van der Weel MJ, Wouterlood FG, Witter MP. Multiple anterograde tracing, combining Phaseolus vulgaris leucoagglutinin with rhodamine- and biotin-conjugated dextran amine. J Neurosci Methods. 1994; 51:9–21. [PubMed: 7514701]

Doyle CA, Maxwell DJ. Catecholaminergic innervation of the spinal dorsal horn: a correlated light and electron microscopic analysis of tyrosine hydroxylase-immunoreactive fibres in the cat. Neuroscience. 1991a; 45:161–176. [PubMed: 1684413]

Doyle CA, Maxwell DJ. Ultrastructural analysis of noradrenergic nerve terminals in the cat lumbosacral spinal dorsal horn: a dopamine-beta-hydroxylase immunocytochemical study. Brain Res. 1991b; 563:329–333. [PubMed: 1786546]

Drye RG, Baisden RH, Whittington DL, Woodruff ML. The effects of stimulation of the A5 region on blood pressure and heart rate in rabbits. Brain Res Bull. 1990; 24:33–39. [PubMed: 1968776]

Ellenberger HH, Feldman JL. Origins of excitatory drive within the respiratory network: anatomical localization. Neuroreport. 1994; 5:1933–1936. [PubMed: 7841379]

Fang F, Proudfit HK. Spinal cholinergic and monoamine receptors mediate the antinociceptive effect of morphine microinjected in the periaqueductal gray on the rat tail, but not the feet. Brain Res. 1996; 722:95–108. [PubMed: 8813354]

Fang F, Proudfit HK. Antinociception produced by microinjection of morphine in the rat periaqueductal gray is enhanced in the foot, but not the tail, by intrathecal injection of alpha1-adrenoceptor antagonists. Brain Res. 1998; 790:14–24. [PubMed: 9593804]

Fardin V, Oliveras JL, Besson JM. A reinvestigation of the analgesic effects induced by stimulation of the periaqueductal gray matter in the rat. I. The production of behavioral side effects together with analgesia. Brain Res. 1984a; 306:105–123. [PubMed: 6540613]

Fardin V, Oliveras JL, Besson JM. A reinvestigation of the analgesic effects induced by stimulation of the periaqueductal gray matter in the rat. II. Differential characteristics of the analgesia induced by ventral and dorsal PAG stimulation. Brain Res. 1984b; 306:125–139. [PubMed: 6466968]

Gebhart, GF.; Randich, A. Brainstem modulation of nociception. In: Klemm, WR.; Vertes, RP., editors. Brainstem Mechanisms of Behavior. Willey and Sons; New York: 1990. p. 315-352.

Gerfen, CR.; Sawchenko, PE.; Carlsen, J. The PHA-L anterograde axonal tracing method. In: Heimer, L.; Zaborszky, L., editors. Neuroanatomical Tract-Tracing Methods. Vol. 2. Plenum; New York: 1989. p. 19-47.

Gilbey MP, Coote JH, Macleod VH, Peterson DF. Inhibition of sympathetic activity by stimulating in the raphe nuclei and the role of 5-hydroxytryptamine in this effect. Brain Res. 1981; 226:131–142. [PubMed: 7296285]

Graham BA, Hammond DL, Proudfit HK. Differences in the antinociceptive effects of alpha-2 adrenoceptor agonists in two substrains of Sprague-Dawley rats. J Pharmacol Exp Ther. 1997; 283:511–519. [PubMed: 9353364]

Granata AR, Numao Y, Kumada M, Reis DJ. A1 noradrenergic neurons tonically inhibit sympathoexcitatory neurons of C1 area in rat brainstem. Brain Res. 1986; 377:127–146. [PubMed: 3730849]

Gray EG. Axo-somatic and axo-dendritic synapses of the cerebral cortex: an electron microscope study. J Anat. 1959; 93:420–433. [PubMed: 13829103]

Hagihira S, Senba E, Yoshida S, Tohyama M, Yoshiya I. Fine structure of noradrenergic terminals and their synapses in the rat spinal dorsal horn: an immunohistochemical study. Brain Res. 1990; 526:73–80. [PubMed: 2078819]

Helfert RH, Juiz JM, Bledsoe SC Jr. Bonneau JM, Wenthold RJ, Altschuler RA. Patterns of glutamate, glycine, and GABA immunolabeling in four synaptic terminal classes in the lateral superior olive of the guinea pig. J Comp Neurol. 1992; 323:305–325. [PubMed: 1360986]

Henderson LA, Keay KA, Bandler R. Hypotension following acute hypovolaemia depends on the caudal midline medulla. Neuroreport. 1998; 9:1839–1844. [PubMed: 9665612]

Hokfelt T, Elde R, Johansson O, Terenius L, Stein L. The distribution of enkephalin-immunoreactive cell bodies in the rat central nervous system. Neurosci Lett. 1977a; 5:25–31. [PubMed: 19604966]

Hokfelt T, Ljungdahl A, Terenius L, Elde R, Nilsson G. Immunohistochemical analysis of peptide pathways possibly related to pain and analgesia: enkephalin and substance P. Proc Natl Acad Sci U S A. 1977b; 74:3081–3085. [PubMed: 331326]

Hokfelt T, Terenius L, Kuypers HG, Dann O. Evidence for enkephalin immunoreactive neurons in the medulla oblongata projecting to the spinal cord. Neurosci Lett. 1979; 14:55–60. [PubMed: 394028]

Holden JE, Proudfit HK. Enkephalin neurons that project to the A7 catecholamine cell group are located in nuclei that modulate nociception: ventromedial medulla. Neuroscience. 1998; 83:929–947. [PubMed: 9483575]

Holden JE, Schwartz EJ, Proudfit HK. Microinjection of morphine in the A7 catecholamine cell group produces opposing effects on nociception that are mediated by alpha1- and alpha2-adrenoceptors. Neuroscience. 1999; 91:979–990. [PubMed: 10391476]

Holtman JR Jr. Marion LJ, Speck DF. Origin of serotonin-containing projections to the ventral respiratory group in the rat. Neuroscience. 1990; 37:541–552. [PubMed: 2133358]

Holtman JR Jr. Speck DF. Substance P immunoreactive projections to the ventral respiratory group in the rat. Peptides. 1994; 15:803–808. [PubMed: 7527143]

Jansen AS, Wessendorf MW, Loewy AD. Transneuronal labeling of CNS neuropeptide and monoamine neurons after pseudorabies virus injections into the stellate ganglion. Brain Res. 1995; 683:1–24. [PubMed: 7552333]

Jensen TS, Yaksh TL. Spinal monoamine and opiate systems partly mediate the antinociceptive effects produced by glutamate at brainstem sites. Brain Res. 1984; 321:287–297. [PubMed: 6149792]

Jensen TS, Yaksh TL. Comparison of antinociceptive action of morphine in the periaqueductal gray, medial and paramedial medulla in rat. Brain Res. 1986; 363:99–113. [PubMed: 3004644]

Jeske I, Reis DJ, Milner TA. Neurons in the barosensory area of the caudal ventrolateral medulla project monosynaptically on to sympathoexcitatory bulbospinal neurons in the rostral ventrolateral medulla. Neuroscience. 1995; 65:343–353. [PubMed: 7539894]

Jones, SL. Descending control of nociception. In: Light, AR., editor. The Initial Processing of Pain and Its Descending Control: Spinal and Trigeminal Systems. Vol. vol. 12. Karger; New York: 1992. p. 203-295.

Keay KA, Clement CI, Owler B, Depaulis A, Bandler R. Convergence of deep somatic and visceral nociceptive information onto a discrete ventrolateral midbrain periaqueductal gray region. Neuroscience. 1994; 61:727–732. [PubMed: 7838371]

Keay KA, Crowfoot LJ, Floyd NS, Henderson LA, Christie MJ, Bandler R. Cardiovascular effects of microinjections of opioid agonists into the ‘Depressor Region’ of the ventrolateral periaqueductal gray region. Brain Res. 1997; 762:61–71. [PubMed: 9262159]

Kwiat GC, Liu H, Williamson AM, Basbaum AI. GABAergic regulation of noradrenergic spinal projection neurons of the A5 cell group in the rat: an electron microscopic analysis. J Comp Neurol. 1993; 330:557–570. [PubMed: 8320344]

Light, AR. The Initial Processing of Pain and Its Descending Control: Spinal and Trigeminal Systems. Karger; Basel: 1992.

Ljungdahl A, Hokfelt T, Nilsson G. Distribution of substance P-like immunoreactivity in the central nervous system of the rat--I. Cell bodies and nerve terminals. Neuroscience. 1978a; 3:861–943. [PubMed: 366451]

Ljungdahl A, Hokfelt T, Nilsson G, Goldstein M. Distribution of substance P-like immunoreactivity in the central nervous system of the rat--II. Light microscopic localization in relation to catecholamine-containing neurons. Neuroscience. 1978b; 3:945–976. [PubMed: 32496]

Loewy AD. Descending pathways to sympathetic and parasympathetic preganglionic neurons. J Auton Nerv Syst. 1981; 3:265–275. [PubMed: 7276435]

Loewy AD, Marson L, Parkinson D, Perry MA, Sawyer WB. Descending noradrenergic pathways involved in the A5 depressor response. Brain Res. 1986; 386:313–324. [PubMed: 3096495]

Loewy AD, McKellar S, Saper CB. Direct projections from the A5 catecholamine cell group to the intermediolateral cell column. Brain Res. 1979; 174:309–314. [PubMed: 487131]

Lovick, T. Interactions between descending pathways from dorsal and ventrolateral periaqueductal gray matter in the rat. In: Depaulis, A.; Bandler, R., editors. The Midbrain Periaqueductal Gray Matter. Plenum Press; New York: 1991. p. 101-120.

Lovick TA. Inhibitory modulation of the cardiovascular defence response by the ventrolateral periaqueductal grey matter in rats. Exp Brain Res. 1992; 89:133–139. [PubMed: 1601091]

Lovick TA. Integrated activity of cardiovascular and pain regulatory systems: role in adaptive behavioural responses. Prog Neurobiol. 1993; 40:631–644. [PubMed: 8484005]

Lyons WE, Grzanna R. Noradrenergic neurons with divergent projections to the motor trigeminal nucleus and the spinal cord: a double retrograde neuronal labeling study. Neuroscience. 1988; 26:681–693. [PubMed: 3173694]

Miller JF, Proudfit HK. Antagonism of stimulation-produced antinociception from ventrolateral pontine sites by intrathecal administration of alpha-adrenergic antagonists and naloxone. Brain Res. 1990; 530:20–34. [PubMed: 1980228]

Milner TA, Pickel VM. Ultrastructural localization and afferent sources of substance P in the rat parabrachial region. Neuroscience. 1986; 17:687–707. [PubMed: 2422594]

Mugnaini, E.; Oertel, WH. An atlas of the distribution of GABAergic neurons and termianls in the rat CNS as revealed by GAD immunohistochemistry. In: Bjorklund, A.; Hokfelt, T., editors. Handbook of Chemical Neuroanatomy. Vol. vol. 4. Elsevier; Amsterdam: 1985. p. 436-608.

Murphy AZ, Ennis M, Rizvi TA, Behbehani MM, Shipley MT. Fos expression induced by changes in arterial pressure is localized in distinct, longitudinally organized columns of neurons in the rat midbrain periaqueductal gray. J Comp Neurol. 1995; 360:286–300. [PubMed: 8522648]

Paxinos, G.; Watson, C. The Rat Brain in Stereotaxic Coordinates. Academic Press; Orlando: 1997.

Peters A, Palay SL. The morphology of synapses. J Neurocytol. 1996; 25:687–700. [PubMed: 9023718]

Peters, A.; Palay, SL.; Webster, dH. Neurons and Their Supporting Cells. Oxford University Press; New York: 1991. The Fine Structure of the Nervous System.

Petrusz, P.; Merchenthaler, I.; Maderdrut, JL. Distribution of enkephalin-containing neurons in the central nervous system. In: Bjorklund, A.; Hokfelt, T., editors. GABA and Neuropeptides in the CNS, Part I. Vol. vol. 4. Elsevier; Amsterdam: 1985. p. 273-334.

Pickel, VM.; Chan, J. Electron microscopic immunocytochemical labeling of endogenous and/or transported antigens in rat brain using silver-intensified one-nanometer colloidal gold. In: Cuello, AC., editor. Immunohistochemistry II. Josh Wiley & Sons; New York: 1993. p. 265-280.

Pickel VM, Joh TH, Reis DJ, Leeman SE, Miller RJ. Electron microscopic localization of substance P and enkephalin in axon terminals related to dendrites of catecholaminergic neurons. Brain Res. 1979; 160:387–400. [PubMed: 33743]

Pickel VM, Towle AC, Joh TH, Chan J. Gamma-aminobutyric acid in the medial rat nucleus accumbens: ultrastructural localization in neurons receiving monosynaptic input from catecholaminergic afferents. J Comp Neurol. 1988; 272:1–14. [PubMed: 2898489]

Proudfit HK. The challenge of defining brainstem pain modulation circuits. J Pain. 2002; 3:350–354. discussion 358-359. [PubMed: 14622736]

Proudfit HK, Clark FM. The projections of locus coeruleus neurons to the spinal cord. Prog Brain Res. 1991; 88:123–141. [PubMed: 1813919]

Proudfit HK, Monsen M. Ultrastructural evidence that substance P neurons form synapses with noradrenergic neurons in the A7 catecholamine cell group that modulate nociception. Neuroscience. 1999; 91:1499–1513. [PubMed: 10391454]

Reichling DB, Basbaum AI. Contribution of brainstem GABAergic circuitry to descending antinociceptive controls: I. GABA-immunoreactive projection neurons in the periaqueductal gray and nucleus raphe magnus. J Comp Neurol. 1990; 302:370–377. [PubMed: 2289975]

Ribak CE, Vaughn JE, Barber RP. Immunocytochemical localization of GABAergic neurones at the electron microscopical level. Histochem J. 1981; 13:555–582. [PubMed: 7031024]

Romagnano MA, Harshbarger RJ, Hamill RW. Brainstem enkephalinergic projections to spinal autonomic nuclei. J Neurosci. 1991; 11:3539–3555. [PubMed: 1658252]

Shults CW, Quirion R, Chronwall B, Chase TN, O'Donohue TL. A comparison of the anatomical distribution of substance P and substance P receptors in the rat central nervous system. Peptides. 1984; 5:1097–1128. [PubMed: 6085163]

Skinner K, Fields HL, Basbaum AI, Mason P. GABA-immunoreactive boutons contact identified OFF and ON cells in the nucleus raphe magnus. J Comp Neurol. 1997; 378:196–204. [PubMed: 9120060]

Smith GS, Savery D, Marden C, Lopez Costa JJ, Averill S, Priestley JV, Rattray M. Distribution of messenger RNAs encoding enkephalin, substance P, somatostatin, galanin, vasoactive intestinal polypeptide, neuropeptide Y, and calcitonin gene-related peptide in the midbrain periaqueductal grey in the rat. J Comp Neurol. 1994; 350:23–40. [PubMed: 7860799]

Stanek KA, Neil JJ, Sawyer WB, Loewy AD. Changes in regional blood flow and cardiac output after L-glutamate stimulation of A5 cell group. Am J Physiol. 1984; 246:H44–51. [PubMed: 6141735]

Van Bockstaele EJ, Branchereau P, Pickel VM. Morphologically heterogeneous met-enkephalin terminals form synapses with tyrosine hydroxylase-containing dendrites in the rat nucleus locus coeruleus. J Comp Neurol. 1995; 363:423–438. [PubMed: 8847409]

Van Bockstaele EJ, Chan J. Electron microscopic evidence for coexistence of leucine5-enkephalin and gamma-aminobutyric acid in a subpopulation of axon terminals in the rat locus coeruleus region. Brain Res. 1997; 746:171–182. [PubMed: 9037496]

Van Bockstaele EJ, Colago EE, Pickel VM. Enkephalin terminals form inhibitory-type synapses on neurons in the rat nucleus locus coeruleus that project to the medial prefrontal cortex. Neuroscience. 1996; 71:429–442. [PubMed: 9053798]

West WL, Yeomans DC, Proudfit HK. The function of noradrenergic neurons in mediating antinociception induced by electrical stimulation of the locus coeruleus in two different sources of Sprague-Dawley rats. Brain Res. 1993; 626:127–135. [PubMed: 7904225]

Westlund KN, Carlton SM, Zhang D, Willis WD. Direct catecholaminergic innervation of primate spinothalamic tract neurons. J Comp Neurol. 1990; 299:178–186. [PubMed: 2229478]

Wouterlood FG, Jorritsma-Byham B. The anterograde neuroanatomical tracer biotinylated dextran-amine: comparison with the tracer Phaseolus vulgaris-leucoagglutinin in preparations for electron microscopy. J Neurosci Methods. 1993; 48:75–87. [PubMed: 7690870]

Yaksh TL. Direct evidence that spinal serotonin and noradrenaline terminals mediate the spinal antinociceptive effects of morphine in the periaqueductal gray. Brain Res. 1979; 160:180–185. [PubMed: 581478]

Yaksh TL, Rudy TA. Narcotic analgestics: CNS sites and mechanisms of action as revealed by intracerebral injection techniques. Pain. 1978; 4:299–359. [PubMed: 25403]

Yeomans DC, Clark FM, Paice JA, Proudfit HK. Antinociception induced by electrical stimulation of spinally projecting noradrenergic neurons in the A7 catecholamine cell group of the rat. Pain. 1992; 48:449–461. [PubMed: 1594267]

Yeomans DC, Proudfit HK. Antinociception induced by microinjection of substance P into the A7 catecholamine cell group in the rat. Neuroscience. 1992; 49:681–691. [PubMed: 1380137]

Zagon A. Internal connections in the rostral ventromedial medulla of the rat. J Auton Nerv Syst. 1995; 53:43–56. [PubMed: 7673601]

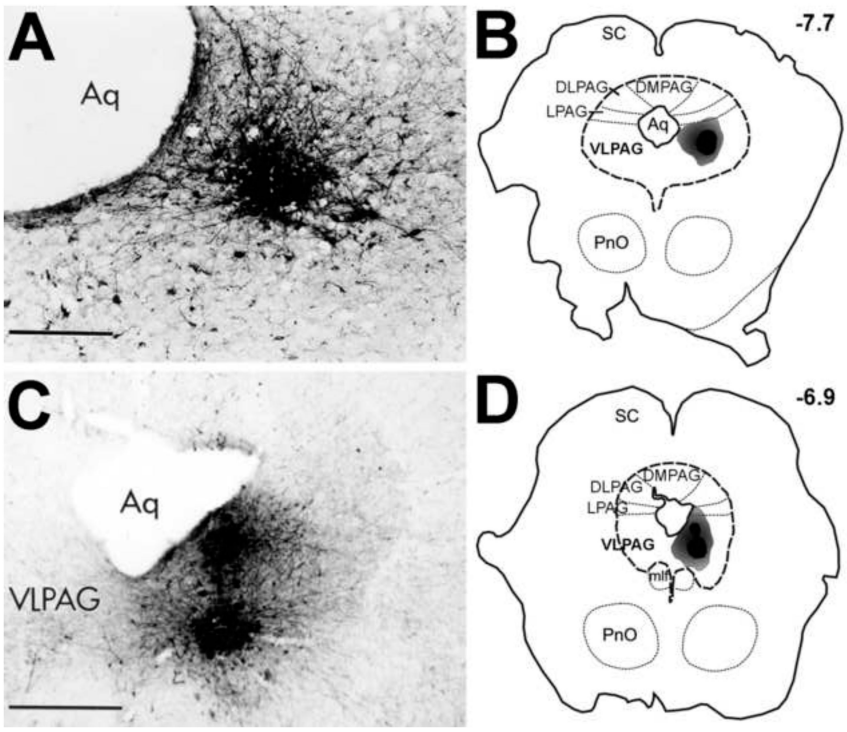

Figure 1. Biotinylated dextran amine (BDA) deposit in the ventrolateral Periaqueductal Gray (VLPAG)

(**A and C**) Photomicrographs of the BDA injection sites in the vlPAG of two cases selected for the ultrastructural analysis. (**B and D**) Schematic drawings illustrate transverse midbrain sections at the level of the superior colliculus (**SC**) that contain a BDA deposit. The solid dark gray area represents a dense core of the tracer deposit, whereas surrounding light gray region represents the area of dense anterogradely-labeled axons. Dashed lines indicate the approximate location of some anatomical landmarks. Numbers in the right upper corners represent distance from Bregma in mm. *Abbreviations:* **Aq**, cerebral aqueduct (Sylvius); D**LPAG**, dorsolateral periaqueductal gray; **DMPAG**, dorsal periaqueductal gray; **LPAG**, lateral periaqueductal gray; **mlf**, medial longitudinal fasciculus; **PnO**, pontine reticular nucleus, oral part. Nomenclature adopted from the adult rat brain atlas (Paxinos and Watson, 1997). Figures are reprints with permission from *Journal of Comparative Neurology* (**A and B**), and *Neuroscience* (**C and D**).

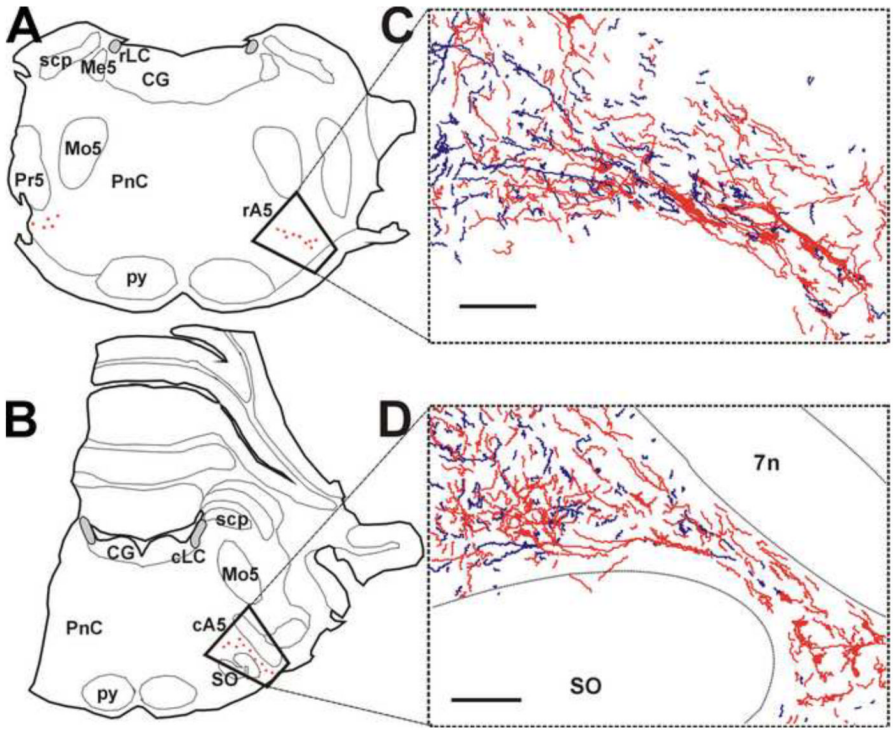

Figure 2. The relationship between BDA-labeled axon terminals and Tyrosine Hydroxylase-immunoreactive (TH-ir) neurons in the A5 cell group

Left panels represent camera lucida drawings of representative transverse pontine sections at the level of the motor nucleus of the trigeminal nerve **(A)** and the superior olive **(B)**. The noradrenergic neurons, represented by red stars, comprise the rostral A5 cell group in the **panel A**, and the caudal A5 cell group in the **panel B**. The areas selected for ultrastructural analysis are enclosed within the trapezoids. Dashed lines identify the approximate location of some anatomical landmarks. **(C and D)** Camera lucida drawings of BDA-labeled axons (blue) and TH-ir profiles (red) in representative transverse pontine sections that include the rostral and the caudal A5 cell groups, respectively. The BDA-labeled axons appear as thin tortuous blue lines, whereas TH-ir neurons and dendrites are represented by red profiles. For photomicrographs and high magnification camera lucida drawings of light-microscopic contacts, please refer to our previous publication (Bajic and Proudfit, 1999). *Abbreviations:* **cA5**, caudal A5 cell group; **CG**, central gray; **cLC**, caudal locus coeruleus; **Me5**, mesencephalic trigeminal nucleus; **Mo5**, motor trigeminal nucleus; **PnC,** pontine reticular nucleus, caudal part; **Pr5**, principal trigeminal nucleus; **py**, pyramidal tract; **rA5**, rostral A5 cell group; **rLC**, rostral locus coeruleus; **scp**, superior cerebellar peduncle; **SO**, superior olive. Scale bars = 200 mm.

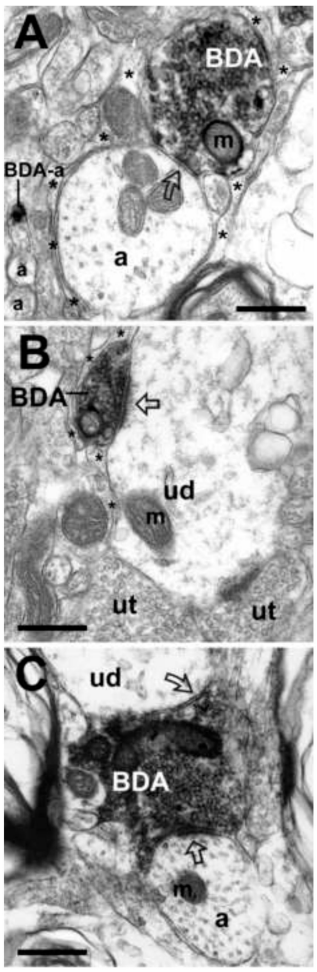

Figure 3. Examples of synapses formed by BDA-labeled axon terminals, originating in the ventrolateral PAG, with unlabeled non-catecholamine profiles in the A5 cell group

(A) Electron micrograph depicts an example of symmetric synapse (open curved arrow) between a BDA-labeled axon terminal (BDA) and an unlabeled axon (a) in the caudal A5 cell group. In the neighboring neuropil, a BDA-labeled axon (BDA-a) is distinguished from unlabeled unmyelinated axons (a). Asterisks denote astrocytic processes. **(B)** Example of an asymmetric synapse (open arrow) characterized by a pronounced post-synaptic density, between a BDA-labeled axon terminal (BDA) containing small clear vesicles, and a medium-sized unlabeled dendrite (ud) in the region of the rostral A5 cell group. The unlabeled dendrite, containing prominent mitochondria (m), is closely apposed to two other unlabeled terminals (ut) containing small clear vesicles. Astrocytic processes (asterisks) envelop non-synaptic areas of both the BDA-labeled terminal and the unlabeled dendrite. **(C)** Example of a BDA-labeled axon terminal (BDA) in the region of the rostral A5 cell group that forms both an asymmetric synapse (open arrow) with an unlabeled axon (a), as well as a symmetric synapse (open curved arrow) with an unlabeled dendrite (ud). Scale bars = 500 nm.

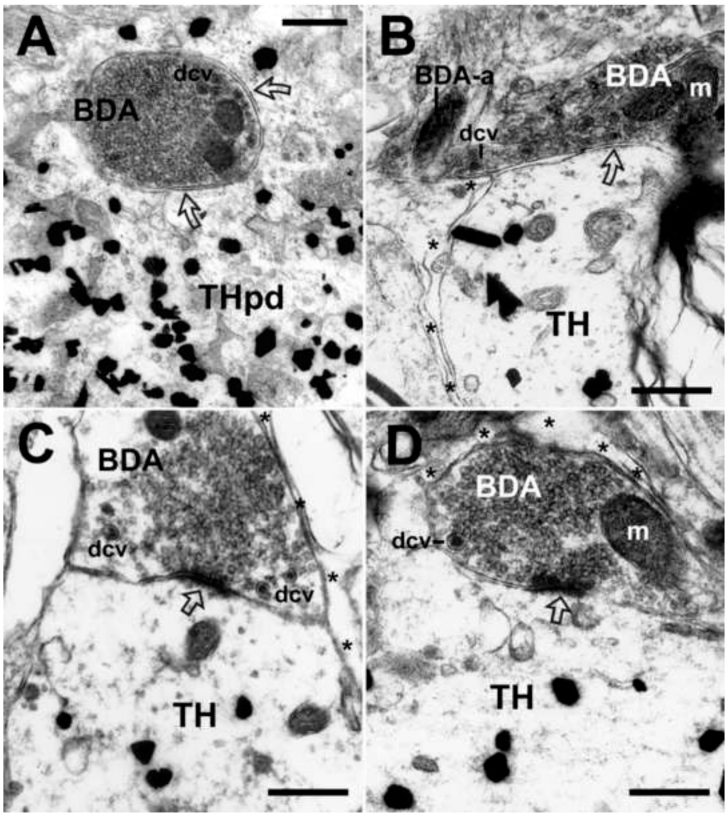

Figure 4. Example of synapses formed by BDA-labeled axon terminals, originating from the ventrolateral PAG, with TH-ir dendrites in the A5 cell group

(A) Electron micrograph illustrates symmetric synapses (open curved arrows) between a lightly BDA-labeled axon terminal (BDA) and a TH-ir proximal dendrite (THpd) in the rostral A5 cell group. The BDA-labeled axon contains small clear vesicles and several dense core vesicles (dcv) near the plasma membrane. **(B)** A BDA-labeled axon terminal (BDA) originating from neuron in the ventrolateral PAG, contains small clear vesicles, several dense core vesicles (dcv) and mitochondria (m), and it forms a symmetric synapse (open curved arrow) with a TH-ir dendrite in the caudal A5 cell group. Astrocytic processes (asterisks) envelop non-synaptic areas of the TH-ir dendrite. Also, unmyelinated BDA-labeled axon (BDA-a) is present in the vicinity of the BDA-labeled axon terminal (BDA). **(C and D)** Panels C and D illustrate examples of asymmetric synapses (open arrows) between the BDA-labeled axon terminals (BDA) originating from neurons in the ventrolateral PAG, and TH-ir dendrites in the rostral A5 cell group. Both anterogradely-labeled terminals are filled with small clear vesicles and contain a few dense core vesicles (dcv) and mitochondria (m). Astrocytic processes (asterisks) envelop non-synaptic areas of both the BDA-labeled terminals and TH-ir dendrites. Scale bars = 500 nm.

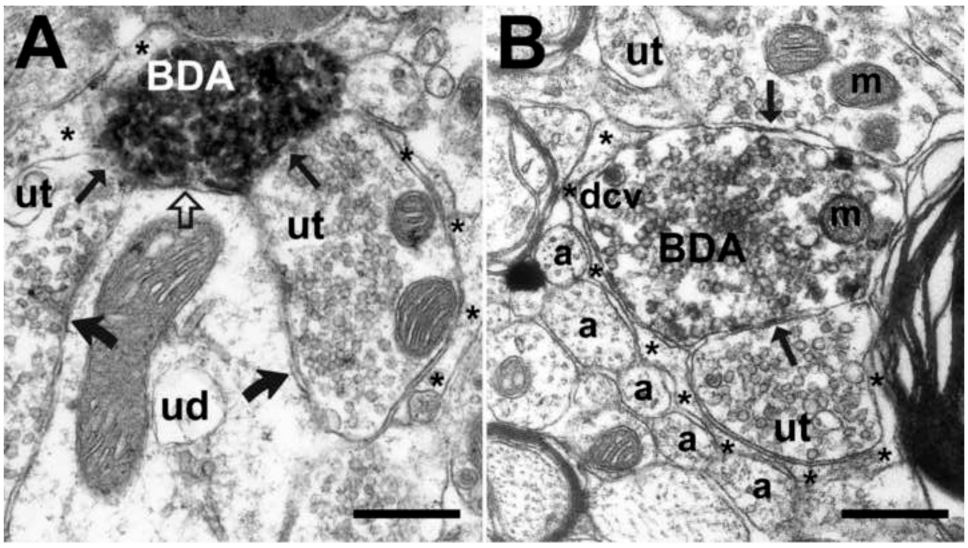

Figure 5. Examples of axoaxonic synapses formed by BDA-labeled axon terminals, originating from neurons in the ventrolateral PAG, with unlabeled axon terminals in the A5 cell group

(A) Illustration of a synaptic arrangement in which BDA-labeled axon terminals (BDA) form axoaxonic appositions (small black arrows) to two unlabeled axon terminals (ut) in the rostral A5 cell group. Both the BDA-labeled (BDA) and the unlabeled terminals (ut) form synapses (open and black curved arrows, respectively) with the same unlabeled dendrite (ud). Astrocytic processes (asterisks) envelop non-synaptic areas. **(B)** Example of a lightly BDA-labeled terminal containing both small clear vesicles (about 15-20 nm in diameter) and dense core vesicles (dcv; about 80-100 nm in diameter) that forms symmetric axoaxonic synapses (small black arrows) with two unlabeled terminals (ut) in the caudal A5 cell group. Astrocytic processes (asterisks) envelop non-synaptic areas of the axon terminals separating them from a group of unlabeled, unmyelinated axons (a). Scale bars = 500 nm.

TABLE 1

Frequency (n) of BDA-labeled Profiles in the A5 Cell Group

	BDA-labeled unmyelinated axons		BDA-labeled myelinated axons		BDA-labeled terminals		Total number
	n	%	n	%	n	%	n
Rostral A5	152	**45**	62	**18**	127	**37**	**341**
Caudal A5	121	**56**	26	**12**	70	**32**	**217**
Total A5	273	**50**	88	**16**	197	**35**	**558**

Values indicate the total numbers (n) of BDA-labeled profiles identified in the rostral and caudal A5 cell group in all sections examined in two animals with nearly identical BDA deposits in the ventrolateral PAG (Fig. 1). The numbers of labeled profiles are also expressed as a percentage of the total counted number of labeled profiles in the rostral A5, caudal A5 and total A5 cell group.

TABLE 2

Contacts by BDA-labeled Terminals in the A5 Cell Group

	BDA/ud		BDA/TH-ir		BDA/ut		BDA/?d		Total
	n	%	n	%	n	%	n	%	n
Rostral A5	86	**43**	16	**8**	90	**45**	9	**4**	201
Caudal A5	35	**38**	9	**10**	43	**47**	5	**5**	92
Total A5	121	**41**	25	**8.5**	133	**45.5**	14	**5**	293

Values indicate the numbers (n) of identified BDA-labeled terminals that formed contacts with several types of postsynaptic profiles including (1) unlabeled dendrites (ud), (2) tyrosine hydroxylase-immunoreactive (TH-ir) neurons and dendrites, and (3) unlabeled axon terminals (ut). Contacts are defined as plasmalemmal appositions and synapses that were formed by BDA-labeled terminals with different types of postsynaptic profiles. The numbers of labeled profiles are also expressed as a percentage of the total number of counted profiles in the rostral A5, caudal A5 and total A5 cell group. A total number of 293 plasmalemmal contacts (synapses and appositions) formed by 197 BDA-labeled terminals were identified in the samples from the A5 cell group. In the rostral A5 cell group, a total number of 127 identified BDA-labeled terminals formed a total number of 201 contacts (synapses and appositions) with different postsynaptic profiles. Similarly, in the caudal A5 cell group, a total number of 70 identified BDA-labeled terminals formed a total number of 92 contacts with postsynaptic profiles. Only 5% (14 out of 293) of the contacts were formed with dendrites that could not be unambiguously identified (?d). For total number of BDA-labeled terminals per subdivision of the A5 cell group, see Table 1.

TABLE 3

Synaptic Contacts of BDA-labeled Terminals

	BDA / unlabeled dendrites						Total ud	BDA / TH-ir dendrites						Total TH-ir	Total # contacts
	apposition		symmetric synapse		asymmetric synapse			apposition		symmetric synapse		asymmetric synapse			
	n	%	n	%	n	%	n	n	%	n	%	n	%	n	n
rA5	58/86	67	18/86	**21**	10/86	**12**	86	8/16	**50**	5/16	**31**	3/16	**19**	16	102
cA5	24/35	69	11/35	**31**	0	**0**	35	7/9	**78**	2/9	22	0	**0**	9	44
Total A5	82/121	**68**	29/121	**24**	10/121	**8**	121	15/25	**60**	7/25	**28**	3/25	**12**	25	146

Summary of Synapses and Plasmalemmal Appositions Between BDA-labeled Terminals with Either Unlabeled Dendrites (ud) or Tyrosine Hydroxylase Immunoreactive (TH-ir) profiles in the A5 cell group. Values indicate numbers of symmetric synapses, asymmetric synapses, and plasmalemmal appositions formed by BDA-labeled terminals (BDA) with different postsynaptic profiles in the rostral (rA5) and caudal (cA5) subdivisions of the A5 cell group. Total numbers of synapse types and plasmalemmal appositions formed by BDA-labeled terminals are also expressed as a percent of the total number of counted BDA-labeled terminal contacts.